NASA Technical Memorandum 82676

Factors Influencing the Predicted Performance of Advanced Propeller Designs

Lawrence J. Bober
Lewis Research Center
Cleveland, Ohio

and

Li-Ko Chang
Purdue University
West Lafayette, Indiana

Prepared for the
Seventeenth Joint Propulsion Conference
cosponsored by the AIAA, SAE, and ASME
Colorado Springs, Colorado, July 27-29, 1981

NASA

FACTORS INFLUENCING THE PREDICTED PERFORMANCE OF ADVANCED PROPELLER DESIGNS

Lawrence J. Bober*
NASA Lewis Research Center
Cleveland, Ohio

and

Li-Ko Chang**
Purdue University
West Lafayette, Indiana

ABSTRACT

The assumptions on which conventional propeller aerodynamic performance analyses are based can be seriously violated when advanced high speed propellers are analyzed. Studies have been performed using a lifting line representation for the propeller to determine the sensitivity of predicted propeller performance to various assumptions in the analysis. Items which have been studied include the method of determining blade section lift and the effects of blade section drag, camber and blade sweep. The effects of nonuniform flow into the propeller and compressibility have also been studied. Comparisons of analytical and experimental results are presented to demonstrate the overall validity of the results.

INTRODUCTION

The recent interest in the turboprop for aircraft propulsion at Mach numbers up to 0.8 has resulted in experimental propeller configuration (Ref. 1) drastically different from those in use on current production aircraft. These advanced propeller concepts have 8 or 10 highly swept blades which operate in a radially varying flow field caused by highly contoured spinners and nacelle. Classical propeller theory is based on the work of Goldstein (Ref. 2) which assumes lightly loaded propellers with straight blades having optimum radial loading distribution. These assumptions are clearly inconsistent with the characteristics of the propellers being studied for high speed applications. The inaccuracies in analytically predicted performance due to these assumptions have not been previously determined.

---

* Aerospace Engineer, Member AIAA

** Aerospace Research Engineer

AIAA Paper No. 81-1564

New analysis methods have been developed which more accurately model the unique characteristics of advanced high speed propellers. These analyses have been described previously in Reference 3. This paper presents results from two lifting line analyses which demonstrate the sensitivity of predicted propeller performance to various simplifying assumptions which can be made in the development of a propeller performance analysis. Analytical results for propeller performance are compared to experimental results to demonstrate the overall validity of the analyses. Since both of the analyses are still under development, these comparisons are not intended to determine which analysis method is better but to indicate the current status of the development efforts.

ANALYSIS METHODS

Method A

This approach is based on the analysis presented in References 4 and 5, which has been extended to include the effects of blade drag and camber and radially varying inflow into the propeller. Each propeller blade is represented by a bound vortex with radially varying strength. This radially varying strength causes vorticity to be shed from the blade and transported downstream forming a helical vortex sheet. In practice the bound vortex is divided into a finite number of elements, each having constant vorticity with a shed vortex filament originating from each filament end point. Each shed vortex is assumed to be a helix with constant pitch. The general method of solution is outlined in Figure 1(a). The radial variation of inflow velocity is determined from a separate analysis of the flow around the nacelle with no blades present. The strengths of the bound vortex elements are determined by requiring that the flow be tangent to the blade at certain control points. The bound vortex elements are placed along the one quarter chord line and an equal number of control points are placed along the three quarter chord line. The influence of the bound and shed vortices at the control points are determined using the Biot-Savart relationship resulting in a series of simultaneous linear equations which are solved for the strengths of the bound vortex elements. This then defines the strength of the shed vortex filaments. The induced flow at the lifting line is then calculated from the known vortex strengths and is added to the propeller inflow velocity and rotational velocity to determine the total velocity. This is then used to determine the lift at each vortex element from the Kutta-Joukowski relationship. This procedure is not valid for elements operating beyond the stall point. The blade drag is then determined from a correlation based on blade camber, thickness, Mach number, and lift (Ref. 6). The lift and drag are resolved into thrust and torque

components which are integrated in a radial direction to determine propeller performance.

Method B

This method, as used in this study, is a simplified version of the approach described in Reference 6. It has been simplified so that it is as consistent as possible with Method A. Method B also uses a finite number of bound vortex elements located along the one quarter line together with shed vorticity downstream of the blade. The major difference between these two approaches is that Method B does not use tangency at control points to close the equations but instead uses two-dimensional airfoil data to relate lift to the induced flow at the lifting line. Each wake vortex was assumed to be a rigid helix with constant pitch, but in the computer program was represented by a series of straight line segments. The general method of solution is outlined in Figure 1(b). The influence of the bound and shed vortices at the lifitng line are determined using the Biot-Savart relationship. A linearized lift slope curve is obtained from data at each bound element and is introduced to relate the vortex strength (lift) to the induced flow (angle of attack). This then results in a set of simultaneous linear equations which can be solved for the strengths of the bound vortex elements. The angle of attack for each element is determined from the induced velocity at the lifiting line, the propeller inflow and rotational velocities and the blade geometric properties. The element lift and drag are then determined from two dimensional airfoil data. An iteration procedure is used to account for nonlinear lift versus angle of attack curves. This also allows the calculation of propeller performance when portions of the blade are operating beyond the stall point if two-dimensional airfoil data is available for this operating range. The lift and drag are resolved into thrust and torque components which are integrated in a radial direction to determine propeller performance.

PROPELLER DESCRIPTION

The methods described above have been used to predict the performance of two 8 blade propellers whose blade planforms are shown in Figure 2. The SR2 blade has no sweep along the midchord line while the SR3 has approximately 45 degrees of sweep along the midchord at the tip.

Additonal geometric characteristics of these two blades are shown in Figure 3. These characteristics define the blade at static (non-rotating) conditions. For swept propeller blades, centrifugal forces cause the blade twist to change. Results

from a finite element structural analysis of the SR3 blade at rotating and non-rotating conditions are shown in Figure 4. The rotating blade curve was obtained at a rotational speed of 8440 rpm which corresponds to the propeller design point advanced ratio of 3.06 and free stream Mach Number of 0.8. These results indicate a maximum change in twist of nearly two degrees due to centrifugal effects. For the results shown subsequently in this paper, at rotational speeds other than the design value, the change in twist was taken to be proportional to the rotational speed squared.

The spinners used with these propellers were designed integrally with the propellers and as such were different for the two propellers. The spinners and nacelle were highly contoured to reduce compressibility losses on the inboard portion of the blades and as such had an appreciable effect on the velocities in the propeller disk. An axisymmetric, transonic, potential flow analysis which includes boundary layer effects (Ref. 7) was used to calculate the flow around the spinner and nacelle with no blades present. The velocity at the lifting line divided by the free stream velocity is shown in Figure 5 at a free stream Mach number of 0.8 for the SR2 and SR3 spinner and nacelle. The higher velocity towards the tip for the SR3 configuration is the result of blade sweep which locates the blade tip further aft relative to the SR2 blades. Thus, the SR3 tip is located above a convex portion of the nacelle resulting in higher velocities than for the SR2 blade tip. Both of these propellers were designed to operate at an advance ratio of 3.06 at a free stream Mach number of 0.8.

RESULTS

Straight Blade Propeller

The effect of camber on predicted propeller performance is shown in Figure 6 for the straight blade SR2 propeller with a blade angle at a radial location of 0.75 times the tip radius (blade angle at 3/4 radius) equal to 58.0 degrees. The free stream Mach number was specified as 0.01 to eliminate compressibility effects and the inflow to the propeller was taken to be uniform (no nacelle effect). Blade drag was taken to be zero. Results are shown from both method A and method B for propeller efficiency and power coefficient as a function of advance ratio. Both methods predict about the same effect due to camber over the entire range of advance ratio. Including camber causes a nearly uniform increase of about 0.06 over the advance ratio range of 3.0 to windmill (power coefficient equal to zero) and about a 0.5 percent decrease in efficiency at an advance ratio of 3.0 becoming negligible at windmill. More important is the difference between the two methods for the no camber cases. For these cases the methods should be equivalent except for the way the lift for each element is determined.

Slightly different methods of representing the wake and determining wake influence coefficients in the two computer programs were compared using a single element and were found to give essentially the same results. The difference between the two methods thus appears to be caused by the different approaches used to obtain the lift. Using two-dimensional airfoil data, Method B, gives higher lift and power coefficient results than using the Kutta-Joukowski relationship, Method A, to get the lift. This is consistent with results obtained for finite wings (Ref. 8) using similar approaches. The efficiency obtained using Method B is up to 3 percent lower at an advance ratio of 3.0 than that obtained using Method A. This trend is consistent with the observed power difference.

Figure 7 presents the effect of free stream Mach number on predicted propeller performance for the SR2 propeller. The effect of camber is included. With zero blade drag, Figure 7(a), the results from Method A indicate no effect of Mach number since the Kutta-Joukowski relationship does not include compressibility effects. The Method B results, however, show a significant effect of Mach number on both power coefficient and efficiency resulting from the Mach number effect in the airfoil data. Increasing the Mach number from 0.01 to 0.8 causes an increase in power coefficient of 0.08 at an advance ratio of 3.0 and a decrease of 0.08 near the windmill point. The same Mach number increase causes a 1 percent decrease in efficienty at an advance ratio of 3.0. The change in efficiency gradually decreases as advance ratio increases, becoming negligible at the windmill point. When blade drag is included, figure 7(b), both methods shown an effect of Mach number since Method A uses Mach number dependent airfoil data to determine the drag. The increase of Mach number from 0.01 to 0.8 now causes an increase in power coefficient at an advance ratio of 3.0 equal to 0.04 for Method A and 0.12 for Method B. The effect of this Mach number change on power coefficient near the windmill point is negligible. The same Mach number increase causes about an 8 percent decrease in efficiency at an advance ratio of 3.0 for both methods.

The effect of drag can be determined by comparing Figures 7(a) and 7(b). While drag has a small effect on power coefficient (about 0.06 increase) it has a very large effect on efficiency. Including drag at a free stream Mach number of 0.8 causes a decrease in predicted efficiency of about 12 percent at an advance ratio of 3.0. Near windmill including drag causes the efficiency to drop from near 100 percent to below zero.

Operating a propeller in the radially varying flow field caused by an axisymmetric nacelle affects the propeller performance as shown in Figure 8. Results are for the SR2 propeller operating in a uniform velocity field and in the nonuniform field shown in Figure 5. Blade camber and drag are included. The effect of non-uniform inflow is similar for both methods. At an advance ratio of 3.0, including nonuniform inflow results in an increase in power coefficient of 0.12 for Method A and an increase of 0.18 for Method B. The efficiency increases about 3 percent for both methods at the same condition. Near the windmill point, power coefficient is insensitive to the change in inflow conditions used here but the efficiency shows a large increase due to nonuniform inflow. The increase in both efficiency and power coefficient at the lower advance ratios is apparently due to a more efficient radial distribution of loading on the blades with the nonuniform inflow.

The validity of the preceding results can be demonstrated by comparing the predicted propeller performance to experimental results. Presented in Figure 9 is such a comparison for the SR2 propeller at a free stream Mach number of 0.8. Blade camber and drag and nonuniform inflow effects are included. Experimental results are unpublished data from the tests decribed in Reference 9. Efficiencies shown in Figure 9 are apparent efficiencies and are higher than the net efficiencies normally shown. Net efficiencies are lower since they account for the increased nacelle drag caused by the inviscid interaction of the operating propeller with the nacelle. The results shown in Figure 9 for power coefficient indicate that Method B more accurately predicts the shape of the data power coefficient but Method A more accurately predicts the level over the range of advance ratio from 3.0 to windmill. The additional set of data at a blade angle of 59.0 degrees is shown merely to demonstrate sensitivity to blade angle. At low Mach numbers with zero blade drag, both methods had approximately the same shape for the power coefficient versus advance ratio curve (Figure 7(a)). Introducing Mach number effects through the airfoil data in Method B, howver, caused a change in slope about equal to the difference in slope of the two curves shown in Figure 9. Therefore, the differences between the two methods with regard to power coefficient appear to result from the Mach number effect on lift although a small difference due to the basic approach for obtaining lift (Figure 6) also exists. Method A slightly overpredicts the efficiency near the design point (J = 3.06) while Method B slightly underpredicts the efficiency. At advance ratios approaching the windmill point Method A more accurately predicts the efficiency.

Propeller efficiency depends on both the level of the power and the radial distribution of aerodynamic load on the blade. A comparison of predicted and measured blade loading distribution

is shown in Figure 10 for the SR2 propeller at a free stream Mach number of 0.8 and an advance ratio of 3.06. The experimental values of elemental power coefficient were determined from steady state flow angle, total pressure and total temperature measurements approximately 1.0 root chord lengths downstream of the root trailing edge. This measurement is independent of the overall performance measurements and as such does not have the same overall performance as shown in Figure 9. Also, since the probe is located some distance downstream of the propeller, any blade wake rollup would cause the measured loading distribution in the wake to be different from the actual loading distribution on the blade. This is however, the only data taken which gives an indication of the radial distribution of loading and as such is presented here. In Figure 10 the Method A results in general agreement better than the Method B results with the data for the same blade angle. However, if the propeller blade were deforming due to aerodynamic or centrifugal loads, then it is possible these results could change. In spite of the differences between the results from the two methods, they do adequately provide an overall description of the loading distribution.

Swept Blade Propeller

Most of the preceding results for the straight blade SR2 propeller are also applicable to the swept blade propeller. Additional results for the SR3 propeller are included in subsequent figures.

The effect of nonuniform inflow on the predicted performance for the SR3 propeller at a free stream Mach number of 0.8 is shown in Figure 11. Blade camber and drag and the centrifugal effect on twist are included. Results indicate a much smaller effect of the nonuniform inflow than for the SR2 propeller. In the outer portion of the propeller where much of the power is absorbed, the SR3 propeller has an average inflow velocity much closer to free stream than the SR2 propeller (Fig. 5) implying that the small effect shown is reasonable. The Method A results indicate approximately a 0.03 increase in power coefficient over the advance ratio range from 3.0 to windmill. At an advance ratio of 3.0, Method A results indicate a 2.0 percent increase in efficiency while Method B results indicate about a 1.5 percent increase in efficiency due to nonuniform inflow.

Comparison of Figure 11 and Figure 8 shows that the difference in slope of the power coefficient curve from the two methods for the SR2 propeller resulting from the Mach number effect on lift is not present in the SR3 results. In both methods the lift is determined based on conditions normal to the lifting

line so that for the swept blade the lift is determined for a much lower Mach number than for the swept blade. For the swept blade the normal Mach numbers should be below drag divergence so that the lift is not appreciably different from the incompressible value.

The magnitude of the centrifugal loading effect on twist, included in Figure 11, is shown in Figure 12. Blade camber and drag and nonuniform inflow effects are included. The centrifugal loading effects on power coefficient are larger than any other effects shown previously. Both methods show about the same decrease in power coefficient due to centrifugal load effects ranging from about 0.36 at an advance ratio of 3.0 to about 0.22 near windmill. Predicted efficiency increases due to centrifugal load effects at an advance ratio of 3.0 are about 4.0 percent for both methods. Near the predicted windmill point there is a large efficiency decrease due to the centrifugal effects.

The SR3 results including blade camber and drag, nonuniform inflow and centrifugal load effect on twist are compared to experimental data in Figure 13. Both methods overpredict the power coefficient although Method A more accurately predicts the level. Both methods deviate further from the data at both high and low advance ratios and are most accurate in the midrange. The assumed variation of twist change with rotational speed affects the shape of the power coefficient curve. The assumed variation with rotational speed squared may be responsible for some of the discrepancy in the predicted and measured power coefficient results. For the efficiency Method A adequately agrees with the data while Method B considerably underpredicts the efficiency at low advance ratios and considerably overpredicts the efficiency at high advance ratios. The differences between the results from the two methods appear to be primarily due to the different approaches used for obtaining lift.

Comparisons for radial distribution of loading are shown in Figure 14 for the SR3 propeller at a free stream Mach number of 0.8 and an advance ratio of 3.06. The Method B results accurately predict the loading distribution over most of the blade, deviating appreciably only in the outer 20 percent of the blade. Method B overpredicts the loading inboard and underpredicts outboard, both by appreciable amounts. Due to the uncertainties in the data noted previously it is not possible to conclude which method more accurately predicts the loading distribution.

Additional features applicable to high speed propellers are contained in the analysis (Ref. 6) of which Method B is a part. Some of these are distorted wake effects including tip rollup, wake compressibility effects through limited regions of influence, supersonic tip corrections to isolated airfoil data, and cascade data for the high solidity portions of the blades. Additional studies are required to determine which of these are appropriate for the prediction of high speed propeller performance.

CONCLUDING REMARKS

A lifting line representation for propeller blades has been employed to determine the sensitivity of predicted high speed propeller performance to various assumptions in the analysis. Two methods for determining the lift along the lifting line have been investigated. One method uses the Kutta-Joukowski relationship to determine lift directly from the lifting line strength while the other uses two-dimensional airfoil data to determine the lift using the induced angle of attack. Differences resulting from these assumptions were identified but neither method was clearly superior. The effects of blade camber and drag, nonuniform inflow to the propeller, free stream Mach number, and centrifugal loads on twist were investigated for both a straight and a swept blade propeller. For the straight blade propeller the nonuniform inflow had the largest effect on predicted power coefficient. For the swept blade propeller the centrifugal load effects on blade twist distribution had the largest effect on predicted power coefficient. For both propellers blade drag had the largest effect on predicted efficiency. Comparisons with experimentally measured propeller performance demonstrated the overall validity of the results and also indicated the need for additional refinements in the analyses.

SYMBOLS

b	chord, ft
C_{LD}	design lift coefficient
C_P	power coefficient, power/$(\rho_\infty n^3 D^5)$
D	propeller diameter, ft.
J	advance ratio, $V_\infty/(nD)$
M_∞	free stream Mach number
n	propeller rotational speed, rps
R	propeller tip radius, D/2, ft.
r	radial location, ft.
t	blade thickness, ft.
V	propeller inflow velocity, fps
V_∞	free stream velocity, fps
$\beta_{3/4}$	blade angle at radial location equal to 3/4 tip radius
$\Delta\beta$	blade twist distribution relative to $\beta_{3/4}$
η	predicted efficiency, (thrust x V_∞)/power
η_{app}	apparent efficiency
ρ_∞	free stream density, lb sec^2/ft^4

REFERENCES

1. R. J. Jeracki, D. C. Mikkelson and B. J. Blaha, "Wind Tunnel Performance of Four Energy Efficient Propellers Designed for Mach 0.8 Cruise", NASA TM-79124, 1979 or SAE Paper 790573, April, 1979.

2. S. Goldstein, "On the Vortex Theory of Screw Propellers", Royal Society (London) Proceedings, Vol. 123, No. 792, Apr. 6, 1929, pp. 440-465.

3. L. J. Bober and G. A. Mitchell, "Summary of Advanced Methods for Predicting High Speed Propeller Performance", NASA TM-81409 or AIAA Paper 80-0225, January, 1980.

4. L. K. Chang, "The Theoretical Performance of High Efficiency Propellers", Ph.D. Thesis, Purdue University, December 1980.

5. J. P. Sullivan, "The Effects of Blade Sweep on Propeller Performance", AIAA Paper 77-716, June 1977.

6. T. A. Egolf, O. L. Anderson, D. E. Edwards, and A. J. Landgrebe, "An Analysis for High Speed Propeller-Nacelle Aerodynamic Peformance Prediction; Volume 1, Theory and Initial Application and Volume 2, User's Manual for the Computer Program", United Technologies Research Center, East Hartford, CT, R79-912949-19, June, 1979.

7. W. L. Chow, L. J. Bober and B. H. Anderson, "Numerical Calculation of Transonic Boattail Flow", NASA TN D-7984, 1975.

8. B. W. McCormick, Jr., "Aerodynamics of V/STOL Flight", Academic Press, New York, 1967, pp 51-71.

9. D. C. Mikkelson and G. A. Mitchell, "High Speed Turboprops for Executive Aircraft-Potential and Recent Test Results", NASA TM-81482, April 1980.

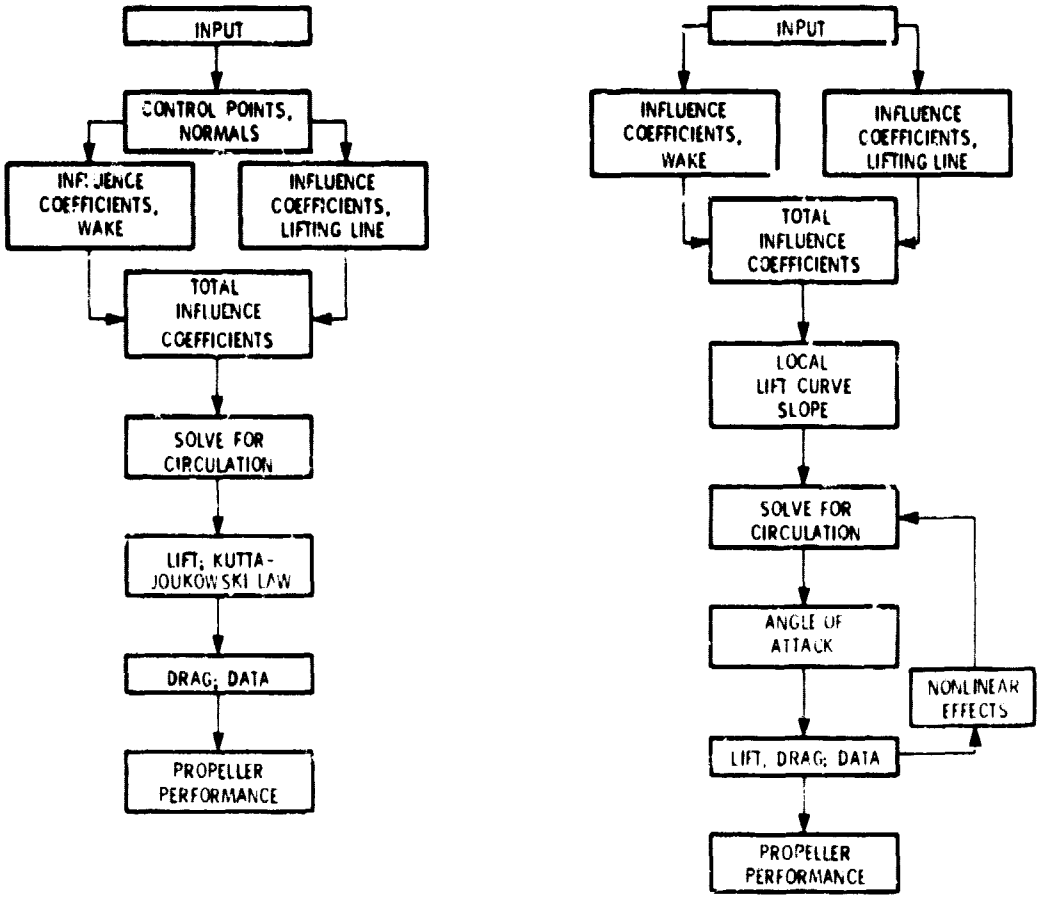

(a) Method A (ref. 2).

(b) Method B (ref. 3).

Figure 1. - Summary of approaches used in present study of aerodynamic performance of advanced high-speed propellers.

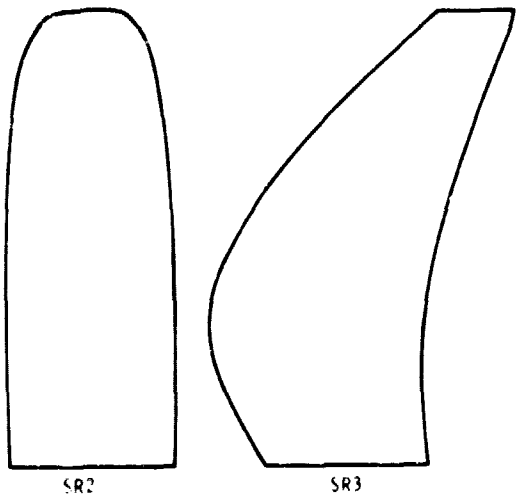

Figure 2. - Blade planform shapes for propellers used in present study.

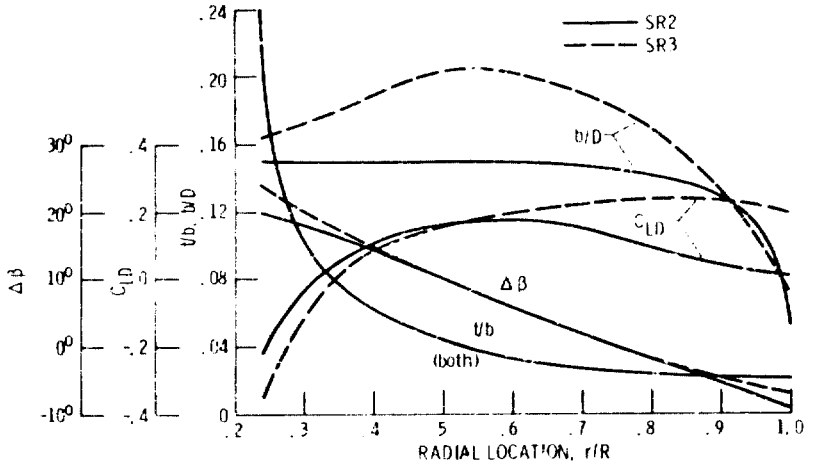

Figure 3. - Blade geometry for propellers used in present study.

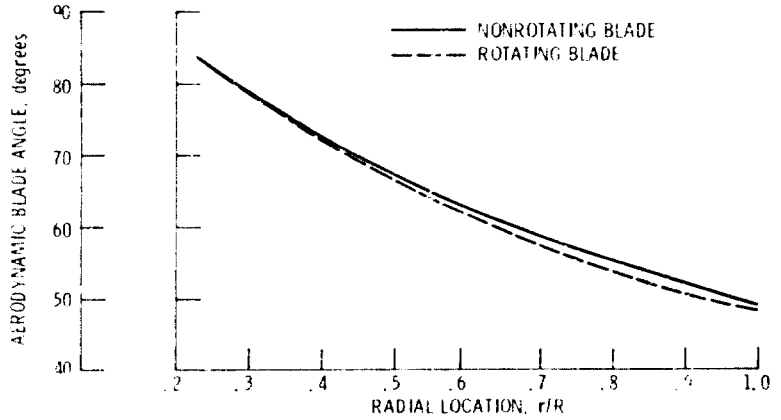

Figure 4. - Effect of centrifugal force on blade twist distribution for swept SR3 propeller blades. Rotational speed = 8440 rpm corresponding to advance ratio of 3.06 at a free stream Mach number of 0.8.

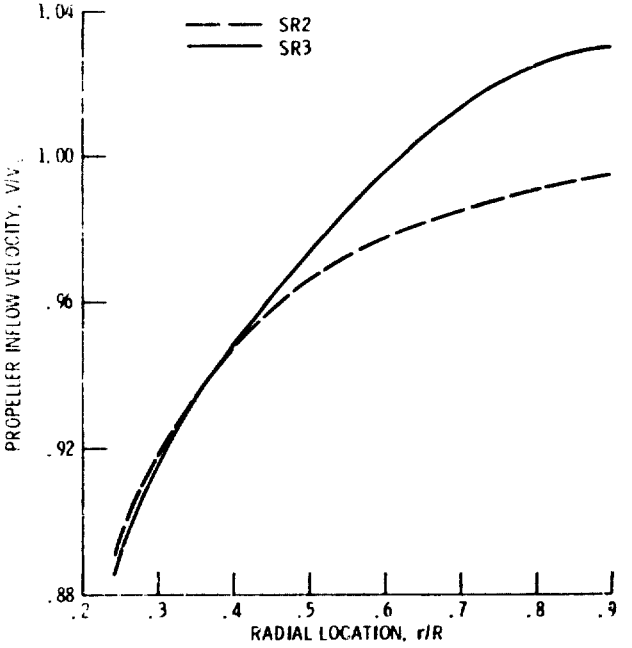

Figure 5. - Nonuniform inflow velocity due to countoured nacelles. Free stream Mach number = 0.8.

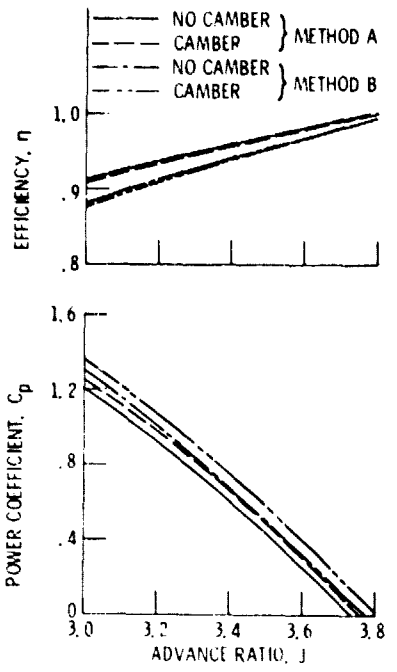

Figure 6. - Effect of camber on predicted propeller performance for SR2 propeller. M_∞ = 0.01, blade drag equals zero, blade angle at 3/4 radius = 58.0, uniform inflow.

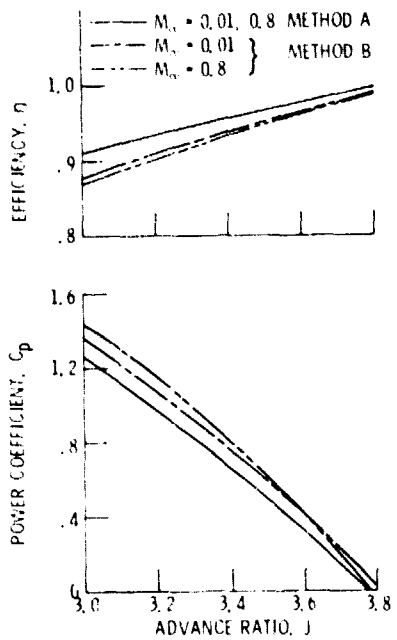

(a) Blade drag equals zero.

Figure 7. - Effect of free stream Mach number on predicted propeller performance for SR2 propeller. Camber effect included, blade angle at 3/4 radius equals 58.0°, uniform inflow.

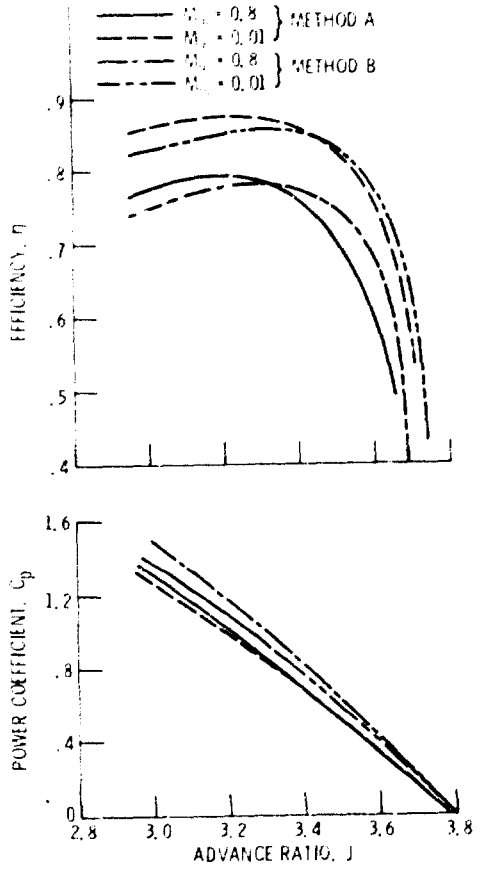

(b) Blade drag included.

Figure 7. - Concluded.

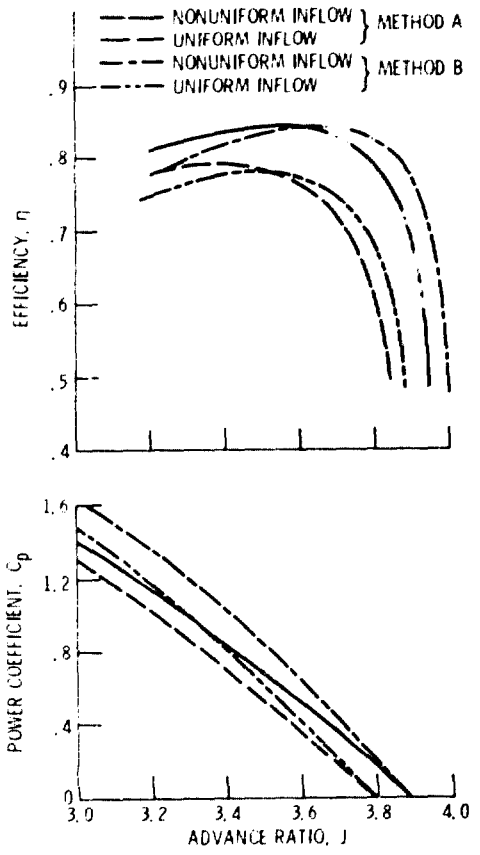

Figure 8. - Effect of nonuniform inflow on predicted propeller performance for SR2 propeller. Camber effect included, blade angle at 3/4 radius equals 58.0°, blade drag included, free stream Mach number equals 0.8.

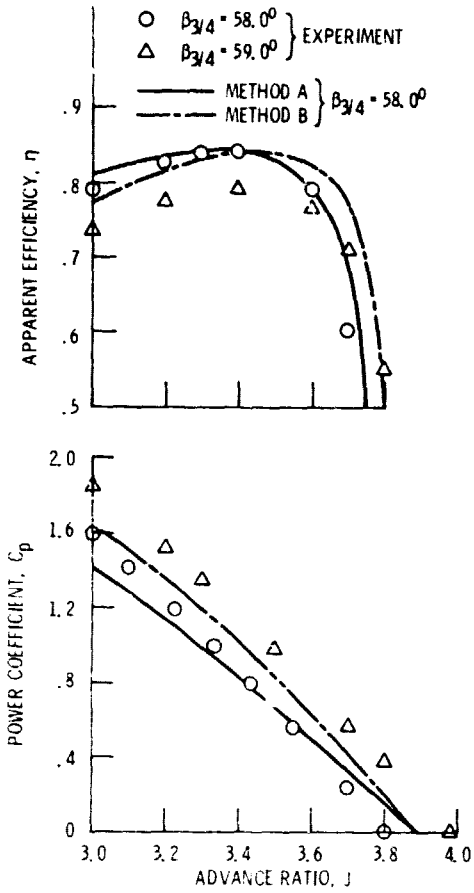

Figure 9. - Comparison of analytical and experimental propeller performance for SR2 propeller at free stream Mach number of 0.8. Camber, drag and nonuniform inflow effects included.

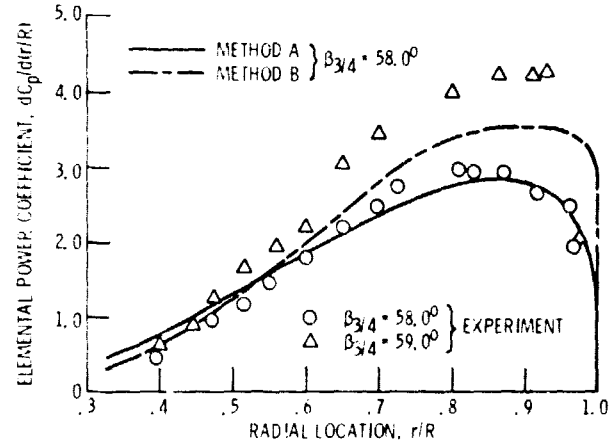

Figure 10. - Comparison of analytical and experimental power loading distribution for SR2 propeller at free stream Mach number of 0.8. Camber, drag and nonuniform inflow effects included, advance ratio equals 3.06.

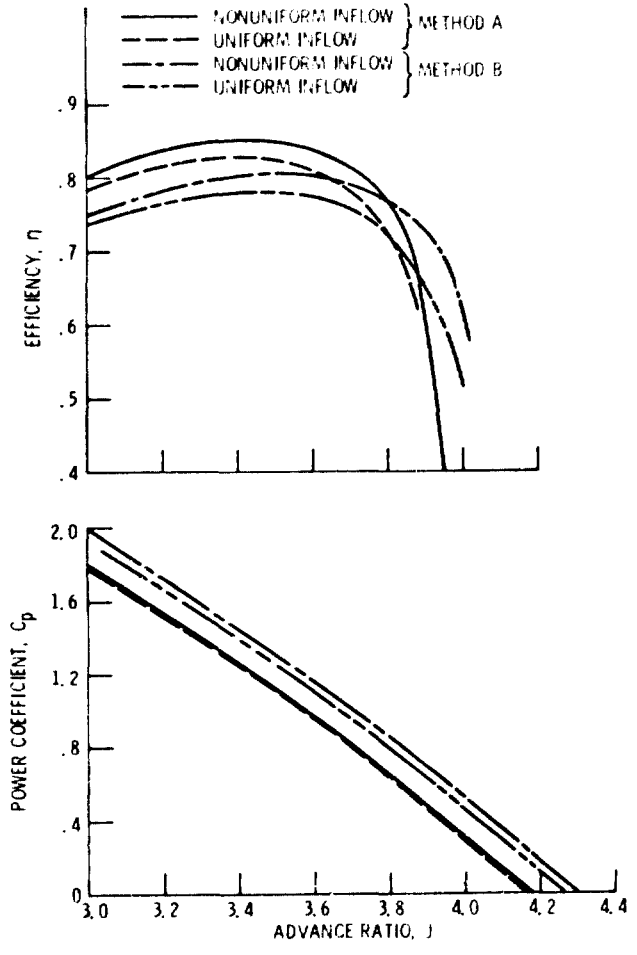

Figure 11. - Effect of nonuniform inflow on predicted propeller performance for SR3 propeller. Free stream Mach number equals 0.8, blade angle at 3/4 radius equals 60.4°. Camber, drag and centrifugal effect on twist included.

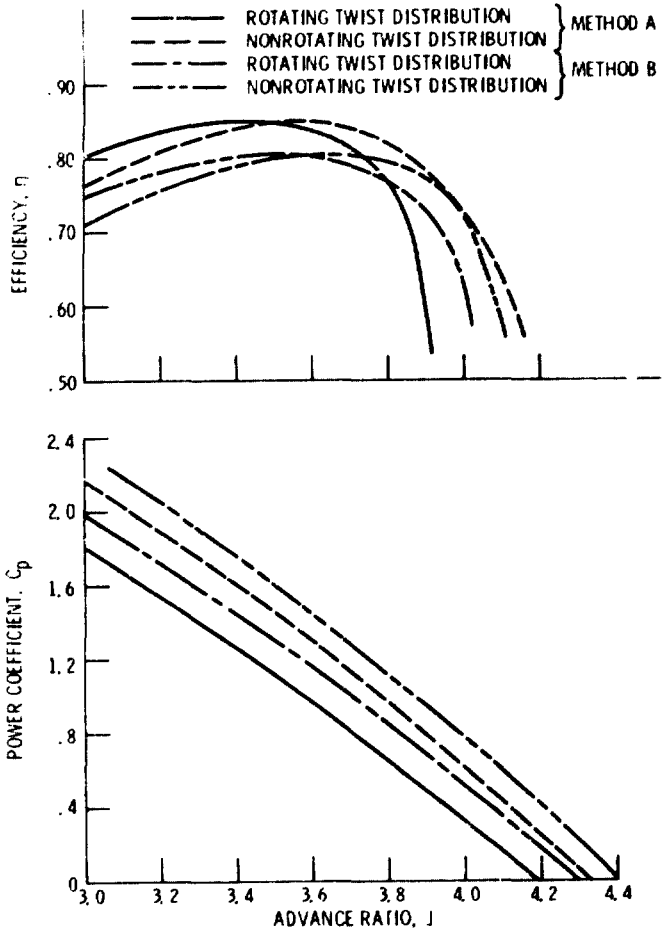

Figure 12. - Effect of modified geometry due to centrifugal loads on propeller performance for SR3 propeller at free stream Mach number equals 0.8. Camber, drag and nonuniform inflow effects included. Blade angle at 3/4 radius equals 60.4°.

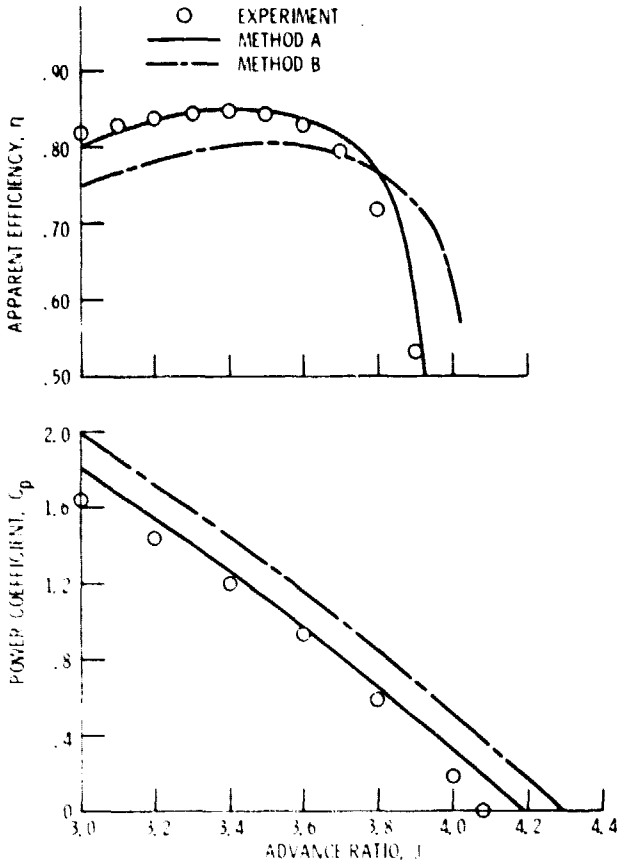

Figure 13. - Comparison of analytical and experimental propeller performance for SR3 propeller at free stream Mach number of 0.8. Camber, drag, nonuniform inflow and centrifugal effect on twist included. Blade angle at 3/4 radius equals 60.4°.

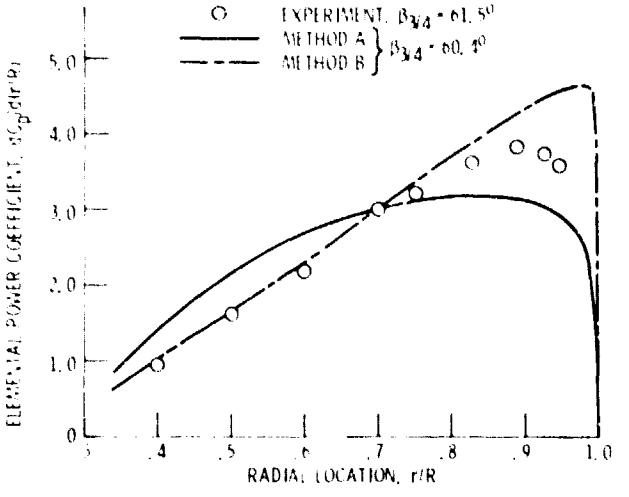

Figure 14. - Comparison of analytical and experimental power loading distribution for SR3 propeller at free stream Mach number of 0.8. Camber, drag, nonuniform inflow and centrifugal effect on twist included. Advance ratio equals 3.06.